ELSEVIER

Nuclear Instruments and Methods in Physics Research A 482 (2002) 832–839

NUCLEAR INSTRUMENTS & METHODS IN PHYSICS RESEARCH Section A

www.elsevier.com/locate/nima

Gamma-ray flux in the Fréjus underground laboratory measured with NaI detector

H. Ohsumi[a,*], R. Gurriarán[a,1], Ph. Hubert[a], R. Arnold[b], C. Augier[c], J. Baker[d], A. Barabash[e], O. Bing[b], V. Brudanin[f], A.J. Caffrey[d], J.E. Campagne[c], E. Caurier[b], D. Dassie[a], V. Egorov[f], K. Errahmane[c], R. Eschbach[a], T. Filipova[f], J.L. Guyonnet[b], F. Hubert[a], C. Jollet[a], S. Jullian[c], I. Kisel[f], A. Klimenko[f], O. Kochetov[f], V.N. Kornoukhov[e], V. Kovalenko[f], V. Kuzichev[e], D. Lalanne[c], F. Laplanche[e], F. Leccia[a], I. Linck[b], C. Longuemare[g], Ch. Marquet[b], F. Mauger[g], H.W. Nicholson[h], I. Nikolic-Audit[a], F. Piquemal[a], J.L. Reyss[i], X. Sarazin[c], A. Smolnikov[f], I. Štekl[j], J. Suhonen[k], C.S. Sutton[h], G. Szklarz[c], V. Timkin[f], V. Tretyak[f], V. Umatov[e], L. Vála[j], I. Vanyushin[e], A. Vareille[a], V. Vasiliev[e], S. Vasiliev[f], V. Vorobel[l], Ts. Vylov[f]

[a] *CENBG, IN2P3-CNRS et Université de Bordeaux I, 33175 Gradignan, France*
[b] *IReS, IN2P3-CNRS et Université Louis Pasteur, 67037 Strasbourg, France*
[c] *LAL, IN2P3-CNRS et Université de Paris-Sud, 91405 Orsay, France*
[d] *INEEL, Idaho Falls, ID 83415, USA*
[e] *ITEP, 117259 Moscow, Russia*
[f] *JINR, 141980 Dubna, Russia*
[g] *LPC, IN2P3-CNRS et Université de Caen, 14032 Caen, France*
[h] *MHC, South Hadley, MA 01075, USA*
[i] *LSCE, CNRS, 91190 Gif sur Yvette, France*
[j] *CTU FNSPE, Prague, Czech Republic*
[k] *JYVÄSKYLÄ University, 40351 Jyväskylä, Finland*
[l] *Charles University, Prague, Czech Republic*

NEMO Collaboration

Received 5 February 2001; received in revised form 21 May 2001; accepted 27 July 2001

Abstract

The γ-ray flux in the Fréjus underground laboratory has been studied using an NaI detector surrounded by different diagonostic shields. Below 4 MeV, the spectrum is dominated by radioactivities in the surrounding materials and rocks. Between 4 and 6 MeV, the shape of the spectrum is well explained by U, Th and daughters, which are internal

*Corresponding author. Address for correspondence: Faculty of Culture and Educations, Saga University, Saga 840-8502, Japan. Fax: +81-952-28-8323.

E-mail addresses: ohsumi@phys.pd.saga-u.ac.jp (H. Ohsumi), rodolfo.gurriaran@ipsn.fr (R. Gurriarán).

[1] Permanent address: IPSN/LRME, 91400 Orsay, France.

PII: S0168-9002(01)01866-6

contaminations in the NaI crystal. Between 6 and 10 MeV, the γ-ray flux is strongly correlated with neutron captures in the surrounding materials. Finally, the γ-ray flux above 10 MeV falls off and is related to the very weak cosmic muon flux via muon bremsstrahlung.

PACS: 29.90.+r; 23.40.−s

Keywords: γ-ray flux; NaI detector; Underground laboratory; Background; Neutron capture γ-ray; Double beta decay

1. Introduction

During the last 10 years, the NEMO Collaboration has been studying the very rare process of double beta (ββ) decay. Two successive prototypes of tracking detectors associated with β-ray calorimeters (NEMO 1 [1] and NEMO 2 [2]) were constructed and ran for a few years in the Fréjus underground laboratory (or Laboratoire Souterrain de Modane, LSM), at a depth of 4800 mwe. Finally, the construction of the NEMO 3 detector, whose aim is the study of Majorana neutrino mass in the order of 0.1 eV, is going on in the LSM.

The half-lives of the neutrinoless double beta ($\beta\beta(0\nu)$) decay are expected to be very long (greater than 10^{24} years). Therefore, all background components must be well identified and the corresponding intensities must be measured. At first, the effect of natural radioactivities was carefully investigated using both the NEMO 2 data and extensive Monte-Carlo calculations, especially in the energy region of the $Q_{\beta\beta}$ values (around 3 MeV) [3]. However, we rapidly realized that neutron and high energy ($\geqslant$4 MeV) γ-ray fluxes could give important contributions in the energy region of the $\beta\beta(0\nu)$ signal. These background components have been studied in Ref. [4].

This paper reports on the γ-ray flux measurement in the LSM using a large volume sodium iodide (NaI) scintillator. Since NaI is sensitive to both γ-rays and neutrons we used different shielding configurations to extract the pure γ-ray flux. Since the expected counting rate is very low, the present experiment has been carried out for more than 3 years.

In the following sections we describe the experimental setup, the γ-ray spectra, the internal U, Th contributions, the effect of neutrons and cosmic rays. Finally, the γ-ray fluxes for different energy domains are given.

2. Experimental arrangement and γ-ray spectra

A large volume NaI scintillator was used for the present γ-ray measurements with three different shielding configurations. The NaI (thallium activated) crystal has a hexagonal cross-section (7.55 cm on a side) and a length of 20.3 cm. The crystal was manufactured by BICRON. It has a cylindrical optical quartz window 7.62 cm in diameter, and 1.27 cm thick that is coupled to an EMI PM tube.

In the first measurement, the crystal was set on a table without any shield. For the second measurement, a neutron shield made with 8 cm borated polyethylene (BPE, 3.5% boron in weight) was used. For the last measurement we used a γ-ray shield made of 5 cm copper and 10 cm lead on the outside (Pb + Cu).

Table 1 summarizes the complete data collection, the shielding condition, and the energy region of the measurements. Each measurement lasted over several months to obtain good statistics in the high energy region. At first, this energy region had a limit of 32 MeV. However, the energy deposit in

Table 1
Summary of experimental searches

Type of shield	Duration (h)	Energy region (MeV)
No shield	6281	0–32
BPE	5476	0–32
Pb + Cu	10 370	0–32
Pb + Cu	4128	0–100

the crystal due to a through going cosmic muon is around 80 MeV. Therefore, we ran the fourth measurement with the NaI crystal inside the Pb + Cu shield but with an upper limit on the energy of 100 MeV.

Fig. 1 shows the NaI energy spectra with the different shielding configurations. They are normalized to the same running time (5476 h).

These spectra can be easily divided into four energy regions as follows:

(I) Below 4 MeV with typical γ-rays due to natural radioactivities from the surrounding materials.

(II) Between 4 and 6 MeV, the counting rates and spectrum shapes are almost independent of the shielding configurations, and as explained in the following subsections are mainly due to the U, Th contaminations of the crystal.

(III) From 6 to 10 MeV we observed similar spectrum shapes but different in intensities, which will be explained as a neutron effect.

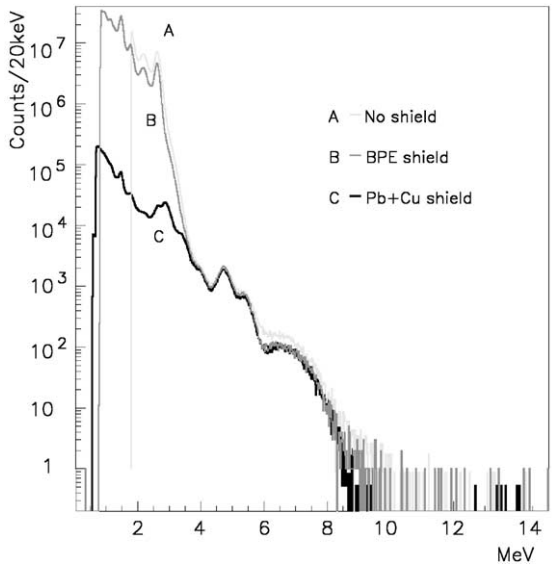

Fig. 1. NaI energy spectra in the LSM with three different shielding configurations. The measuring time is normalized to 5476 h. For the spectrum without shield, the lower threshold was increased up to 2 MeV in order to decrease the counting rate. For these spectra a self-energy calibration was made using the ^{40}K line at 1.46 MeV, the ^{208}Tl line at 2.61 MeV, the 4.7 MeV peak corresponding to the sum of the β decaying ^{212}Bi and the α decaying ^{212}Po, and the maximum energy of the neutron capture γ-rays in copper at 7.9 MeV.

Table 2
Counting rates for the three different shields as a function of energy region. The measurement in the energy region 10–100 MeV was done only with the Pb + Cu shield. Quoted errors are statistical only

Energy region (MeV)	No shield (counts/h)	BPE (counts/h)	Pb + Cu (counts/h)
4–6	19.7(0.1)	18.1(0.1)	16.6(0.1)
6–10	1.99(0.02)	1.34(0.02)	1.25(0.01)
10–32	$11.4(1.3) \times 10^{-3}$	$8.0(1.2) \times 10^{-3}$	$2.6(0.5) \times 10^{-3}$
10–100			$5.5(1.2) \times 10^{-3}$

(IV) Above 10 MeV, the counting rates drop drastically, only the very weak cosmic muon flux inside the laboratory remains.

Table 2 gives the counting rates for each energy region and each shield.

3. External natural radioactivity

Below 4 MeV all the γ-ray spectra are mainly produced by the natural radioactivities in the surrounding materials. Due to the rather poor energy resolution ($\sim$8% at 1 MeV) only a few lines are well identified, i.e., the 1.46 MeV from ^{40}K and the 2.61 MeV from ^{208}Tl. In Table 3, the experimental counting rates of these typical two lines are shown for the two cases: no shield and the Pb + Cu shield. The variation in count rate of the 2.61 MeV line is in perfect agreement with the expected value, 13.0(1) counts/h were recorded in Pb + Cu shield and 12(1) were calculated from the shielding attenuation factors. This demonstrates the external origin of these γ-rays. After a Monte-Carlo (GEANT) simulation of the detector efficiency at

Table 3
Counting rates for the 2.61 MeV (^{208}Tl) and 1.46 MeV (^{40}K) γ-ray lines with and without Pb + Cu shield. Quoted errors are statistical only

Peak energy (MeV)	No shield (counts/h)	Pb + Cu shield (counts/h)
2.61	9743(3)	13.0(1)
1.46	40 487(7)	28.7(1)

this energy, the flux of 2.61 MeV photons was calculated as $I_\gamma(2.61\ \text{MeV}) = 4 \times 10^{-2}\ \text{cm}^{-2}\ \text{s}^{-1}$. This flux is highly dependent on the materials placed near the detector (for example, the type of PM tubes, localization of the electronics). It can be noted that 10 cm of Pb and 5 cm of Cu are not enough to completely suppress this flux. This explains why γ-ray shields are generally made with 15 cm of Pb and a few cm of Cu.

On the contrary, the counting rate variation of the 1.46 MeV line cannot be explained by the attenuation factor alone: 28.7(1) counts/h were recorded with the Pb + Cu shield, while only 15(1) were expected. This indicates some ^{40}K activity inside the shield, most probably from the glass of the PM tube. From the intensity of this line without shielding we can calculate the flux of $I_\gamma(1.46\ \text{MeV}) = 0.1\ \text{cm}^{-2}\ \text{s}^{-1}$.

As shown in Fig. 1, without a shield or with a light BPE shield, the counting rate in the energy interval 2.61–4 MeV decreased by 4 orders of magnitude.

4. Internal background due to α, β decays of U, Th series

Here, we will discuss the intermediate energy region of 4–6 MeV. They are the same structures in the energy region as shown in Fig. 1. Moreover, Table 2 shows that the counting rate is almost unaffected by the presence or absence of any type of shield. This fact means that the counting rate is dominated by the internal activities inside the NaI crystal. There exist numerous reports (for example see Ref. [5]) showing that inorganic scintillators usually contain small concentrations of U, Th and progenies. So we expect the shape of the spectrum to be explained by summed effects of α, β and γ decays.

A Monte-Carlo simulation using GEANT was made, taking into account all possible decays, quenching factors and the above summed effects. Secular equilibrium inside the U and Th chains was assumed. The result is shown in Fig. 2 and compared with the experimental data with the Pb + Cu shield.

Between 4 and 6 MeV the events are mainly due to the β decay of ^{212}Bi followed by the

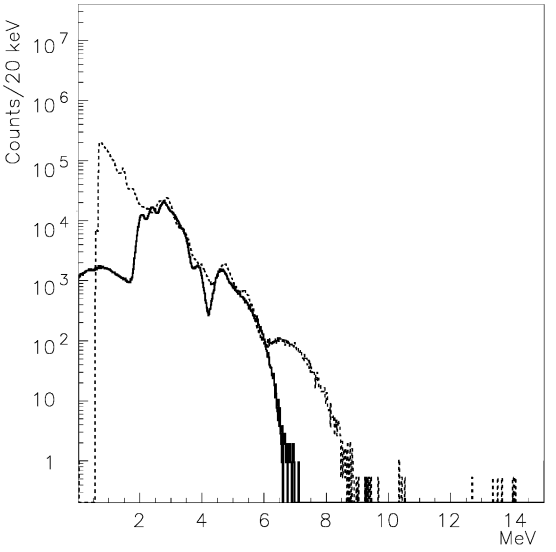

Fig. 2. The energy spectrum due to U and Th series, calculated by the Monte-Carlo simulations (solid line). For comparison, the measured energy spectrum (dashed line) with the Pb+Cu is shown in the same figure.

^{212}Po α decay:

$$^{212}\text{Bi} \xrightarrow{\beta^-} {}^{212}\text{Po} \Rightarrow {}^{208}\text{Po}. \quad Q_\beta = 2.2\ \text{MeV}\ \ T_{1/2} = 0.3\ \mu\text{s}\ \ Q_\alpha = 8.784\ \text{MeV}$$

The summed energy between the β and α decay energies is possible because the scintillation decay constant of the NaI is about 0.25 μs. Here, the quenching factors of α particles in the NaI are assumed to be 0.5, which is in good agreement with the present spectrum. Below 4 MeV the spectrum is given by the β and α decays of both the U and Th series. This component is negligible when compared with the γ-ray flux of natural radioactivity even with a Pb + Cu shield.

Finally, from the comparison between simulated and experimental spectra we have deduced the amount of impurities in the crystal: 0.4 mBq/kg (Th), 0.17 mBq/kg (U), corresponding to 0.1 ppb in Th and 0.014 ppb in U. These values are not so strange contaminations for this type of scintillator.

5. Neutron induced γ-ray events

Here, we will discuss the energy region from 6 to 10 MeV. In this energy domain there is no

contribution from the external natural radioactivity or from internal contamination.

All spectra are similar in shape (Fig. 1) rapidly decreasing up to 10 MeV but with different intensities (Table 2). This behavior suggests an effect of neutrons. This has been verified in a short run with a neutron source a few meters away from the detector. Fig. 3 shows the comparison between γ-ray spectra recorded with the NaI crystal inside the Pb + Cu shield with and without the presence of the neutron source. Note that the spectra are not normalized in time. The running time is 18.2 h in the presence of the source and 10 370 h without the source. Above 6 MeV the shapes are the same and can be explained by neutron captures in the surrounding materials and in the iodine of the NaI crystal. The neutron binding energy of almost all nuclei (Cu, Pb, I, Fe, etc.) is distributed up to 10 MeV and leads to many γ-ray emissions in the 6–10 MeV range.

In order to extract from the data the γ-ray flux between 6 and 10 MeV it is much easier to work on the spectrum recorded with the NaI inside the BPE shield. In this case the counting rate (J) is given by the following equation:

$$J_{\mathrm{BPE}}(6-10\ \mathrm{MeV}) = f_{\mathrm{BPE}} I_{\gamma}(6-10\ \mathrm{MeV}) + g_{\mathrm{BPE}} I_{\mathrm{n}} \quad (1)$$

where I_{γ} (I_{n}) is the γ-ray (neutron) flux in unit of $\mathrm{cm}^{-2}\ \mathrm{s}^{-1}$. The f and g proportional coefficients are as follows.

The f coefficient is the energy average product of three values: (i) the γ-ray detection efficiency, (ii) the γ-ray transmission coefficient through the relevant shielding (BPE in this case), and (iii) the geometrical cross-section of the NaI detector. It is calculated using the GEANT code by simulation of the energy response of the NaI using the geometrical parameters of the detector and of the shield, and using a γ-ray flux (through the whole detector area) randomly generated in the incident direction. The energy distribution of the incident γ-ray flux is assumed to be the same as the experimental energy spectrum of the NaI when located in the BPE shield. The f coefficient then comes directly from the ratio of the number of events recorded in the relevant energy domain to the number of incident γ-ray. Note that the f coefficient is in unit of cm^2. Since the intensity of the incident γ-ray flux is rapidly dropping down as a function of the energy, different shapes (or slopes) have been tried, which have shown effects on the determination of this f coefficient as large as 30%.

The coefficient g (in unit of cm^2) is the product of four values: (i) the transmission coefficient of the neutron through the relevant shield, (ii) the probability of the γ-ray emission after the neutron captures, (iii) the detection efficiency of the emitted γ-rays, and (iv) the geometrical cross-section of the NaI detector. It is calculated in the same way as the f coefficient, but with the addition of the MICAP routine [6,7] to the GEANT code in order to follow the neutrons inside the experimental setup. Different neutron energy distributions were assumed (for example: (1) fast neutron energy distributions from ^{252}Cf fission or Am–Be sources, (2) various distributions with the epithermal neutron energy, (3) thermal neutron with Maxwellian distributions). The uncertainty on g comes

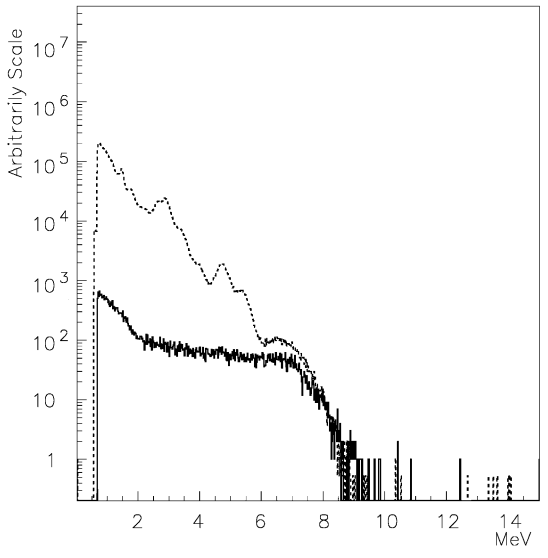

Fig. 3. The energy spectrum (solid line) with a weak neutron source placed during 18.2 h several meters away from the NaI detector with the Pb + Cu shield. For comparison, the background spectrum (dashed line) without the neutron source recorded during 10 370 h is shown in the same figure. The scales have been adjusted to show that the shapes of the spectra are similar between 6 and 10 MeV.

from the γ-ray detection efficiency calculation, the uncertainty on the neutron capture cross-section, and the neutron simulation, whose contributions are also estimated to be as large as 30%.

For this experimental setup with 8 cm BPE around the scintillator, we got $f_{\mathrm{BPE}} = 116\ \mathrm{cm}^2$, and found that the second term in Eq. (1) is completely negligible, since thermal and epithermal neutrons are fully stopped in the shield while the fast neutron flux is strongly suppressed. From the data reported in Table 2 the γ-ray flux between 6 and 10 MeV is $3.2 \pm 1.0 \times 10^{-6}\ \mathrm{cm}^{-2}\ \mathrm{s}^{-1}$.

From the data recorded with the bare NaI (no shield, nsh), we can extract some rough estimation of the neutron flux in the LSM. In this case, the counting rate between 6 and 10 MeV is given by the following equation:

$$J_{\mathrm{nsh}}(6-10\ \mathrm{MeV}) = f_{\mathrm{nsh}} I_{\gamma}(6-10\ \mathrm{MeV}) + g_{\mathrm{nsh}}^{\mathrm{th}} I_{\mathrm{n}}^{\mathrm{nsh}} + g_{\mathrm{nsh}}^{\mathrm{epth}} I_{\mathrm{n}}^{\mathrm{epth}} + g_{\mathrm{nsh}}^{\mathrm{fast}} I_{\mathrm{n}}^{\mathrm{fast}} \quad (2)$$

where $f_{\mathrm{nsh}} = 145\ \mathrm{cm}^2$. In this equation the neutron flux is divided into three components. They are the thermal (th, 0.025 eV), the epithermal (epth, 0.1 eV–100 keV), and the fast neutrons (fast, 100 keV–10 MeV). However, it is known that the capture cross-section for thermal neutrons is much higher than for epithermal neutrons and negligible for fast neutrons. So we expect $g_{\mathrm{nsh}}^{\mathrm{th}} \gg g_{\mathrm{nsh}}^{\mathrm{epth}} \gg g_{\mathrm{nsh}}^{\mathrm{fast}}$. Moreover, from neutron measurements in other underground laboratories [9,10] we do not expect the epithermal neutron flux to be larger than the thermal one. So the last two terms can be neglected. Using the calculated $g_{\mathrm{nsh}}^{\mathrm{th}} = 23\ \mathrm{cm}^2$, the thermal neutron flux is found to be $4 \pm 2 \times 10^{-6}\ \mathrm{cm}^{-2}\ \mathrm{s}^{-1}$. This rough estimation is in reasonable agreement with a previous measurement ($1.6 \pm 0.1 \times 10^{-6}\ \mathrm{cm}^{-2}\ \mathrm{s}^{-1}$) carried out in the LSM using ^{3}He counter [8]. Error on the neutron flux is estimated around 50%, which comes from the uncertainties in the f and g calculations and in the I_{γ}(6–10 MeV) determination.

6. γ-ray flux above 10 MeV

As seen in Fig. 1, the counting rate drops rapidly above 10 MeV. Fig. 4 shows the energy spectra between 10 and 32 MeV for the three different shield configurations. The corresponding counting rates between 10 and 32 MeV are also reported in Table 2. These counting rates are similar with no shield and with a light BPE shield. However, the counting rate with the Pb + Cu shield is about four times less. Even if the setup is located deep underground, the explanation of this data needs to call for cosmic-ray–muon interactions. This is evident from the results shown in Fig. 5 which give the comparison between the energy spectra of NaI up to 100 MeV in the above ground laboratory of Bordeaux and in the LSM. The Bordeaux spectrum was taken with a similar NaI (geometry and PM tube) in triple coincidence with two large plastic scintillators (0.5 m^2, 15 mm thick). We clearly see a bump at 70 MeV, which is consistent with the deposited energy calculated via the GEANT code for the average muon energy of 1 GeV in the above ground laboratory. The difference in the counting rates between the two measurements is more than 6 orders of magnitude which corresponds to the reduction of the muon flux.

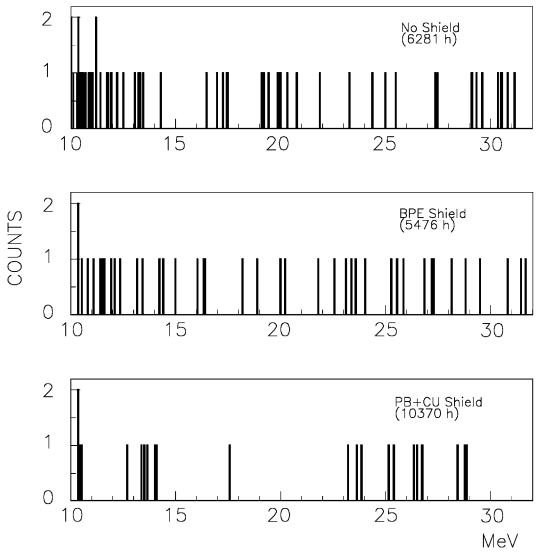

Fig. 4. The NaI energy spectra between 10 and 32 MeV at the LSM with three different shields: no shield (top), BPE shield (center), and Pb + Cu (bottom).

To get an estimate of the muon flux we used again the data recorded up to 100 MeV when the NaI is inside the Pb + Cu shield. Since Pb + Cu is a

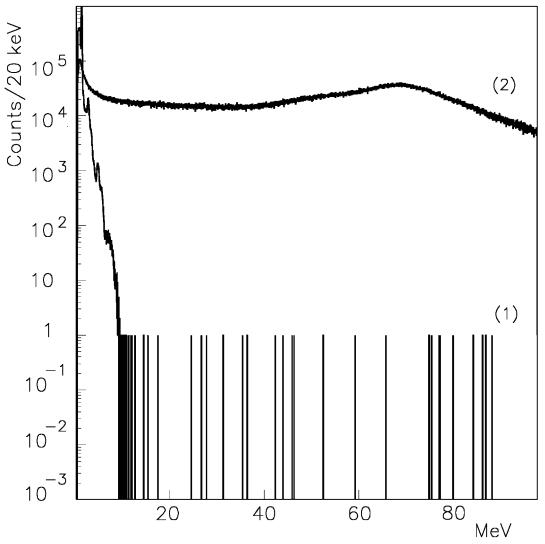

Fig. 5. The energy spectrum (1) of the NaI detector in the LSM up to 100 MeV, compared to the spectrum (2) measured at the overground laboratory in Bordeaux. The measuring time is normalized to 4128 h. The energy calibration of (2) is made using the ^{40}K line at 1.46 MeV and the minimum ionization peak at 70 MeV.

good γ-ray shield the counting rate in this shield above 10 MeV can be interpreted as muon interactions in the NaI. Assuming an average energy of 10 TeV, we simulated with GEANT the experimental conditions and found a muon detection efficiency of 62% between 10 and 100 MeV. This leads to a muon flux of $7.7 \pm 1.7\ \mathrm{m^{-2}\ day^{-1}}$ which is in reasonable agreement with the published value of $4.2\ \mathrm{m^{-2}\ day^{-1}}$ from the proton decay experiment [11].

Now let us come back to the data shown in Fig. 4 and Table 2, between 10 and 32 MeV. From the counting rate with no shield and after subtraction of the data with Pb + Cu, which corresponds to the direct muon component, we are left with a counting rate of around 9×10^{-3} counts/h. This is interpreted as pure γ-rays from muon bremsstrahlung in the surrounding rocks or materials. Such high-energy γ-rays when entering the NaI crystal have nearly a 80% detection efficiency. Therefore, the flux for γ-rays with an energy between 10 and 32 MeV is found to be $1.1 \pm 0.3 \times 10^{-8}\ \mathrm{cm^{-2}\ s^{-1}}$. The 30% error in this case is only statistical.

7. Conclusion

Using a simple experimental device, i.e., a large volume NaI scintillator, we have investigated the γ-ray fluxes in different energy domains in the LSM. Since the NaI crystal is at the same time sensitive to γ-rays and neutrons, it has been necessary to take data with three different shield configurations, they were no shield, BPE and finally Pb + Cu. For a given energy range, and for each shield, the NaI counting rates (J) can be generally expressed with a set of the following equation:

$$J = fI_\gamma + gI_\mathrm{n} + C \tag{3}$$

where the f coefficient is related to the γ-detection efficiency calculated with GEANT, and the g coefficient is related to the γ-ray detection after neutron capture in the NaI or the surrounding materials. g is calculated with the GEANT + MICAP code, assuming a known energy distribution of the I_n flux inside the laboratory. C is a constant related to the background such as natural radioactivities inside the detector or direct interaction of muons with the crystal.

Using reasonable assumptions, the set of equations (3) can be easily solved and the I_γ values extracted for different energy domains. For example, as already said above, for energies higher than 10 MeV there is no effect of neutrons, and the C constant is given by the direct muon flux. Another example is that between 6 and 10 MeV there is no effect of the internal radioactivities, the direct interaction of muon is negligible, and the fast neutron scattering on the crystal can also be neglected since it leads only to low energy γ-rays (<3 MeV).

After the full analysis, the extracted γ-ray fluxes in the LSM are presented in Table 4, and compared with similar measurements made at Broken Hill (1230 mwe Australia) [12]. It should be noted that above 6 MeV the values are rather similar, within a factor of 2, for both underground laboratories. However, below 6 MeV, there is a large difference which can be understood easily due to variations in the internal U, Th, Ra radioactivity levels in different NaI detectors.

Table 4
The γ-ray fluxes in the LSM. The unit of flux is 10^{-6} cm^{-2} s^{-1}. Errors in the present measurements are about 30%. The results of similar measurements made at the Broken Hill underground facility are also shown (see text)

Energy interval (MeV)	LSM (present measurement)	Broken Hill (Ref. [12])
4.0–6.0	3.8	22.5
6.0–7.0	1.5	3.7
7.0–8.0	1.6	0.8
8.0–9.0	0.07	0.14
9.0–10.0	0.05	0.03
> 10.0	0.01	≃ 0.004

These values can be used to investigate the level of background for many underground experiments. The γ-ray flux with energies greater than 10 MeV should be strongly dependent on the depth of the laboratory. However, the γ-ray flux below 10 MeV is dependent on the level of radioactivity of the rocks and surrounding materials, either through direct γ-ray emission or through neutron captures. The neutron flux comes from the U spontaneous fission and/or the (α, n) reactions, and is also correlated to the radioactivity level. Since the average level of radioactivity is nearly the same in almost all underground laboratories, we do not expect strong variations from one laboratory to another one.

With the NEMO 3 experiment in the LSM, we are looking for a signal of ββ(0ν) centered at 3.03 MeV. Simulations of neutron and γ-ray interactions, using the published neutron fluxes [8] and the presently measured γ-ray fluxes, under the optimum shield conditions, have shown that for 5 years of data acquisition the number of events between 2.8 and 10 MeV are 2.5 ± 0.8. In the ββ(0ν) energy domain, from 2.8 to 3.2 MeV for ^{100}Mo, we expect 0.10 ± 0.03 counts in 5 years, which is negligible [4].

Acknowledgements

The authors would like to thank the LSM staff for their technical assistance in running the experiment.

References

[1] D. Dassié, et al., Nucl. Instr. and Meth. A 309 (1991) 465.
[2] R. Arnold, et al., Nucl. Instr. and Meth. A 354 (1995) 338.
[3] R. Arnold, et al., Nucl. Phys. A 636 (1998) 209.
[4] Ch. Marquet, et al., Nucl. Instr. and Meth. A 457 (2001) 487.
[5] A.M. Bakich, et al., Nucl. Instr. and Meth. A 226 (1984) 383 and references therein.
[6] F. Piquemal, et al., private communications, 1999.
[7] C. Zeitnitz, T.A. Gabriel, Nucl. Instr. and Meth. A 349 (1994) 106.
[8] V. Chazal, et al., Astroparticle Phys. 9 (1998) 163.
[9] A. Rindi, et al., Nucl. Instr. and Meth. A 272 (1988) 871; R. Aleksan, et al., Nucl. Instr. and Meth. A 274 (1989) 203.
[10] S.R. Hasemi-Nezhad, L.S. Peak, Nucl. Instr. and Meth. A 357 (1995) 524.
[11] C. Berger, et al., Nucl. Instr. and Meth. A 262 (1987) 463.
[12] G. Braoudakis, L.S. Peak, Nucl. Instr. and Meth. A 332 (1993) 292.